


NEW MATERIALS FOR INFRARED TRANSMITTING ELECTROOPTIC FILTERS

AD-A187 899

Quarterly Technical Report No. 7
For period 1 August 1979 through 30 October 1979
Contract MDA 903-78-C-0180
Program Code Number 8D10
Program Element Code 61101E

Hughes Research Laboratories
3011 Malibu Canyon Road
Malibu, CA 90265

Sponsored by
Defense Advanced Research Projects Agency (DoD)
DARPA Order No. 3519
Monitored by DARPA under Contract MDA 903-78-C-0180


A.L. Gentile
Principal Investigator
(213) 456-6411

DTIC
ELECTE
DEC 03 1987
S
FE

The views and conclusions contained in this document are those of the authors and should not be interpreted as necessarily representing the official policies, either expressed or implied, of the Defense Advanced Research Projects Agency or the U.S. Government.

This document has been approved
for public release and sale; its
distribution is unlimited.

87 11 18 071

ARPA Order Number	3519
Name of Contractor	Hughes Research Laboratories 3011 Malibu Canyon Road Malibu, CA 90265
Effective Date of Contract	1 February 1978
Contract Expiration Date	30 June 1980
Contract Number	MDA 903-78-C-0180
Name and Phone Number of Principal Investigator	A.L. Gentile (213) 456-6411
Contract Period Covered by This Report	1 August 1979 through 30 October 1979

UNCLASSIFIED

SECURITY CLASSIFICATION OF THIS PAGE (When Data Entered)

REPORT DOCUMENTATION PAGE		READ INSTRUCTIONS BEFORE COMPLETING FORM
1. REPORT NUMBER	2. GOVT ACCESSION NO. ADA187899	3. RECIPIENT'S CATALOG NUMBER
4. TITLE (and Subtitle) NEW MATERIALS FOR INFRARED TRANSMITTING ELECTROOPTIC FILTERS		5. TYPE OF REPORT & PERIOD COVERED Quarterly Tech. Rpt. 7 1 Aug 1979 - 30 Oct 1979
7. AUTHOR(s) A.L. Gentile		6. PERFORMING ORG. REPORT NUMBER
9. PERFORMING ORGANIZATION NAME AND ADDRESS Hughes Research Laboratories 3011 Malibu Canyon Road Malibu, CA 90265		8. CONTRACT OR GRANT NUMBER(s) MDA 930-78-C-0180
11. CONTROLLING OFFICE NAME AND ADDRESS Defense Advanced Research Projects Agency 1400 Wilson Boulevard Arlington, VA 22209		10. PROGRAM ELEMENT, PROJECT, TASK AREA & WORK UNIT NUMBERS Program Code No. 8D10 Prog. Element Code 61101E
14. MONITORING AGENCY NAME & ADDRESS (if different from Controlling Office)		12. REPORT DATE November 1979
		13. NUMBER OF PAGES 27
		15. SECURITY CLASS. (of this report) UNCLASSIFIED
		15a. DECLASSIFICATION DOWNGRADING SCHEDULE
16. DISTRIBUTION STATEMENT (of this Report) Approved for public release; distribution unlimited.		
17. DISTRIBUTION STATEMENT (of the abstract entered in Block 20, if different from Report)		
18. SUPPLEMENTARY NOTES Work on this program has been performed by personnel at the Hughes Research Laboratories as well as by Dr. Alexander Borshchevsky, Center for Materials Research, Stanford University, and Professor Paul L. Richards, Department of Physics, University of California at Berkeley.		
19. KEY WORDS (Continue on reverse side if necessary and identify by block number) Electrooptic materials Ternary chalcogenides IR materials "Defect" chalcopyrites Binary chalcogenides		
20. ABSTRACT (Continue on reverse side if necessary and identify by block number) The objectives of this program are to find and develop new IR transmitting materials and to provide new data on the electrooptic (EO) properties of those most likely to have an EO coefficient an order of magnitude higher than materials currently in development for tunable filters. The main technical problems anticipated include the synthesis and single-crystal growth of these materials: many are poorly characterized and others have high melting points or melt incongruently. Our		

UNCLASSIFIED

SECURITY CLASSIFICATION OF THIS PAGE (When Data Entered)

X
UNCLASSIFIED

SECURITY CLASSIFICATION OF THIS PAGE (When Data Entered)

approach will overcome these obstacles by first synthesizing 20 polycrystalline samples; subsequently, dielectric constants at low and ambient temperatures will be determined, and the two best materials of the survey will be grown as single crystals (second year of the program).

During the last quarter, emphasis was placed on the growth of single-crystal CdIn_2Te_4 . Using the published phase equilibrium diagram, the liquid-solid relationships were established for crystal growth. A small single crystal of CdIn_2Te_4 was grown near the end of the quarter. In addition, synthesis of ZnIn_2S_4 was started using the constituent elements but failed to go to completion because a sulfide layer formed on top of the molten metals and prevented further reaction with gaseous sulfur.

Quantitative calculations of EO coefficients were made for ternary compounds and showed close agreement with measured results.

UNCLASSIFIED

SECURITY CLASSIFICATION OF THIS PAGE (When Data Entered)

TABLE OF CONTENTS

SECTION		PAGE
	REPORT SUMMARY	4
1	INTRODUCTION AND SUMMARY	5
	A. Program Objectives	5
	B. Summary	5
2	MATERIALS PREPARATION AND CRYSTAL GROWTH	6
	A. CdIn_2Te_4	6
	B. ZnIn_2S_4	8
3	MATERIALS EVALUATION	11
	A. Properties of CdIn_2Te_4	11
	B. Quantitative Calculation of EO Coefficients	11
	REFERENCES	14
	APPENDIX	15

Accession For	
NTIS GRA&I	<input checked="" type="checkbox"/>
DTIC TAB	<input type="checkbox"/>
Unannounced	<input type="checkbox"/>
Justification	
By	
Distribution/	
Availability Codes	
Dist	Avail and/or Special
A-1	

REPORT SUMMARY

The objectives of this program are to find and develop new IR transmitting materials and to provide new data on the electrooptic (EO) properties of those most likely to have an EO coefficient an order of magnitude higher than materials currently in development for tunable filters. The main technical problems anticipated include the synthesis and single-crystal growth of these materials: many are poorly characterized and others have high melting points or melt incongruently. Our approach will overcome these obstacles by first synthesizing 20 polycrystalline samples; subsequently, dielectric constants at low and ambient temperatures will be determined, and the two best materials of the survey will be grown as single crystals (second year of the program).

During the last quarter, emphasis was placed on the growth of single-crystal CdIn_2Te_4 . Using the published phase equilibrium diagram, the liquid-solid relationships were established for crystal growth. A small single crystal of CdIn_2Te_4 was grown near the end of the quarter. In addition, synthesis of ZnIn_2S_4 was started using the constituent elements but failed to go to completion because a sulfide layer formed on top of the molten metals and prevented further reaction with gaseous sulfur.

Quantitative calculations of EO coefficients, based on the bond charge dielectric theory of Phillips and Van Vechten, were made for ternary compounds and showed good agreement with measured results.

SECTION 1

INTRODUCTION AND SUMMARY

A. PROGRAM OBJECTIVES

The objectives of this program are to find and develop new IR transmitting materials and to provide new data on the electrooptic (EO) properties of those most likely to have EO coefficients an order of magnitude higher than materials currently in development for tunable filters. The main technical problems anticipated include the synthesis and single-crystal growth of these materials: many are poorly characterized and others have high-melting points or melt incongruently. Our approach will overcome these obstacles. First, we will synthesize 20 polycrystalline samples. Then the dielectric constant of each, at both low and ambient temperatures, will be determined, and the two best materials of the survey will be grown as single crystals (second year of the program).

B. SUMMARY

During the last quarter, emphasis was placed on the growth of single-crystal CdIn_2Te_4 . Using the published phase equilibrium diagram, the liquid-solid relationships were established for crystal growth. A small single crystal of CdIn_2Te_4 was grown near the end of the quarter. In addition, synthesis of ZnIn_2S_4 was started using the constituent elements but failed to go to completion because a sulfide layer formed on top of the molten metals and prevented further reaction with gaseous sulfur.

Quantitative calculations of EO coefficients, based on the bond charge dielectric theory of Phillips and Van Vechten, were made for ternary compounds and showed good agreement with measured results.

SECTION 2

MATERIALS PREPARATION AND CRYSTAL GROWTH

A. CdIn_2Te_4

Primary emphasis during this quarter was placed on the growth of single-crystal CdIn_2Te_4 , a compound that we previously had reported¹ as having a high value for the low-frequency dielectric constant. Using the solid-liquid relationships shown (Figure 1) in the pseudo-binary phase diagram $\text{CdTe-In}_2\text{Te}_3$ as published² in the literature, we attempted to grow single-crystal material. Melt compositions were selected lying in the composition range covered by the line a-b. In this region, solid CdIn_2Te_4 ($\beta \equiv \text{solid CdIn}_2\text{Te}_4$) is in equilibrium with liquid in the temperature range 785°C to 702°C. By selecting a starting composition close to "a," crystals of pure CdIn_2Te_4 can be grown by lowering the temperature. Below 702°C, however, additional phases begin to solidify and cause a multiphase polycrystalline region to begin to grow, thus preventing further single-crystal growth.

Several runs were made utilizing the conditions discussed above to grow single-crystal CdIn_2Te_4 . Fused quartz crucibles approximately 16 mm in diameter with conical bottoms were used to nucleate single-crystal growth. The sealed, evacuated ampoules were processed in a vertical two-zone Bridgman-like furnace. The ampoule was rotated and vibrational stirring was applied during the growth cycle. As anticipated from the above discussion, several ingots were produced in which the lower (conical-shaped) sections were single phase and, in one case, a single crystal of CdIn_2Te_4 ; the upper parts were multiphase and polycrystalline.

X-ray microprobe analysis of the single-phase material showed insignificant variations in composition from nose to tail with an average composition:

58% Te

29% In

13% Cd.

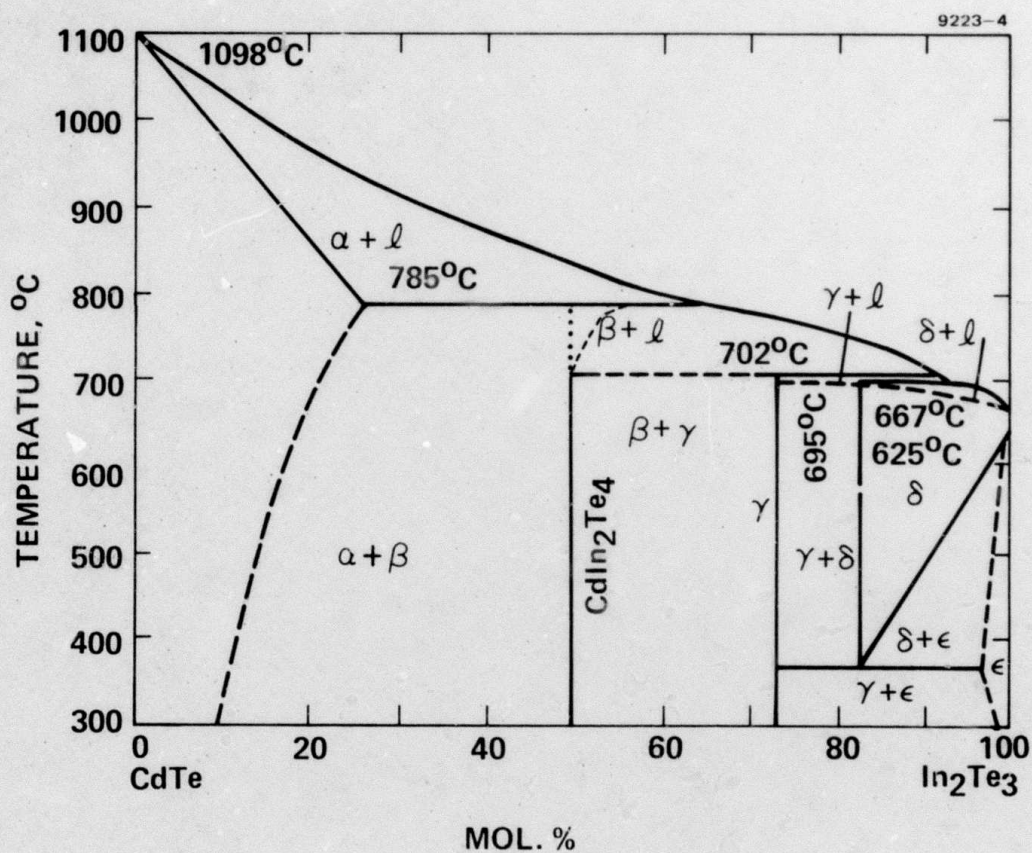


Figure 1. Phase equilibrium diagram for CdTe-In₂Te₃.

There are indications from the analysis that the composition is slightly rich in In_2Te_3 and that there is some solid solubility between CdIn_2Te_4 and In_2Te_3 . However, our results indicate that the solid solubility line between the regions is more vertical than that reported in Ref. 1 (dashed line in Figure 1) and probably closer to the vertical (dotted) line in Figure 1.

One of the most successful ingots from these runs (Figure 2) yielded a single-crystal section (cone-shaped) as well as the final multiphase section; the boundary between the sections is noted in Figure 2. The tip of the cone appears as-grown and indicates a poor start with nucleation getting underway on an apparent gas void, resulting in a concave interface observed during crystallization. That the crystal grew single under these conditions (see Figure 3, SEM photo of as-grown tip), as confirmed by the growth patterns shown in Figure 3 and by Laue patterns, is very encouraging for future single-crystal growth runs.

Plans for the next quarter include further attempts at single-crystal growth of CdIn_2Te_2 seeking optimum temperature-lowering rates to prevent the crystal from cracking as well as solution from being entrapped to obtain the largest high-quality single crystal for evaluation of its EO properties.

B. ZnIn_2S_4

During the last quarter, considerable effort was expended to synthesize ZnIn_2S_4 from its constituent elements: Zn, In, and S. A long-term run in which the molten metals were exposed to gaseous sulfur failed to go to completion after several weeks and was aborted. Subsequent observation indicated that a layer of the sulfide had formed on top of the molten metals and prevented further reaction. A second run has gotten underway with added iodine to initiate vapor transport of the solidified species and allow further reaction to take place.

9298-3

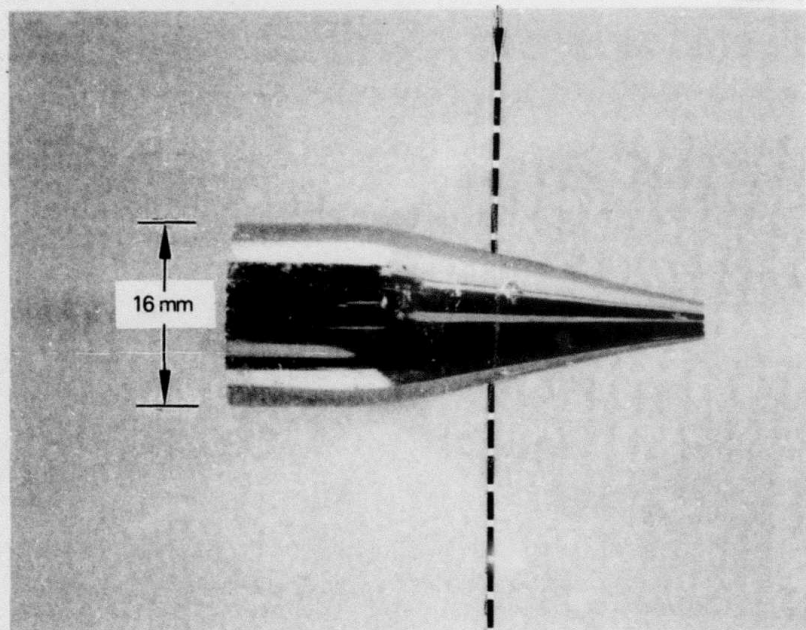


Figure 2. Ingot containing single-crystal CdIn_2Te_4 .
(Region to right of dashed line is single.)

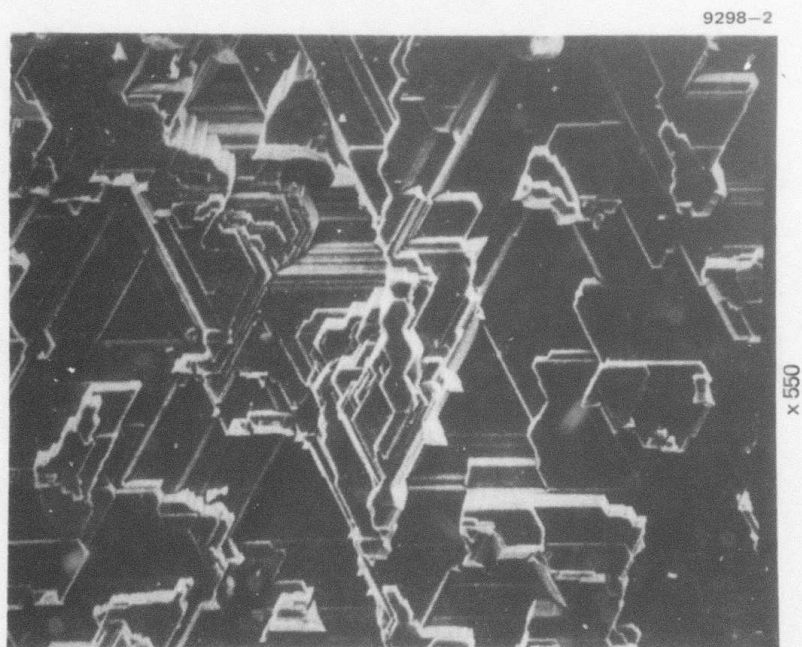


Figure 3. SEM photograph of tip of CdIn_2Te_4 .

SECTION 3
MATERIALS EVALUATION

A. PROPERTIES OF CdIn_2Te_4

CdIn_2Te_4 has been reported³⁻⁷ to have the following properties:

- Crystal class Tetragonal, $\bar{4}$
- Band gap 0.9 eV
- Resistivity (r.t.) Maximum $10^5 \Omega\text{-cm}$ (n type)
 Minimum $60 \Omega\text{-cm}$
- Mobility $4000 \text{ cm}^2 \text{V}^{-1} \text{sec}^{-1}$
- Transmission range 1 to $37 \mu\text{m}$
- Density 5.9 g/cm^3 .

Our measurements indicate that the sample we grew has a resistivity of $10^7 \Omega\text{-cm}$ at room temperature. The dielectric constant at 10 kHz was measured to be 456 at room temperature. Low-temperature measurements showed a significant decrease in dielectric constant to 73 at 83°K. It is possible that CdIn_2Te_4 is a ferroelectric slightly below room temperature. Our evaluation to date has not proven that it is, but there is no definite evidence that it is not. This evaluation is continuing, and our results will be discussed in a future report.

B. QUANTITATIVE CALCULATION OF EO COEFFICIENTS

The following represents the work of Professor Amnon Yariv and his graduate student, C. Shih, of the California Institute of Technology. They have applied the bond charge dielectric theory of Phillips and Van Vechten to the calculation of the EO tensor coefficients. Comparisons with experimental values for binary compounds having zincblende and wurtzite structures (as previously reported, Quarterly Report 4) is very good.

Yariv and Shih recently extended the calculations to ternary compounds e.g., LiNbO_3 , CdIn_2Te_4 , where they also find very good agreement. These results will appear in Table I. A discussion of the calculation appears in the appendix.

We applied the theoretical model for calculating the electrooptic coefficient to the crystal CdIn_2Te_4 . We used the following data:

- Covalent radii ($\text{Cd}_j\text{In}_j\text{Te}$) - 1.405Å
- Structure - $\bar{4}$

Using published data of bond susceptibilities, we calculated the optical dielectric constant $\epsilon_\infty = 7.25$. Using the above data in the equations

$$\begin{aligned}
 (r_{ijk})_{\text{ionic}} &= -\frac{\epsilon_o(\epsilon'_{dck} - \epsilon'_{\infty k})}{V N e_c^* \epsilon'_i \epsilon'_j} \sum_{\mu} \frac{\beta_{\mu}}{r} \left[(f_i \alpha_i^{\mu} \alpha_j^{\mu} \alpha_k^{\mu}) \right. \\
 &\quad \left. + 1/2 (\alpha_i^{\mu} \delta_{jk} + \alpha_j^{\mu} \delta_{ik}) \right] \\
 f &= \left(\frac{k_s r}{2} - 1.48 \right) f_i - 0.02 \quad ,
 \end{aligned} \tag{1}$$

we obtain the result

$$r_{41} = 220 \times 10^{-12} \text{ m/V } \pm 30\% .$$

This predicted value is a huge number (roughly 100X that of GaAs and 10X that of LiNbO_3). The main difference between this crystal and LiNbO_3 , as an example, is due to the factor:

$$\frac{\epsilon_{dc} - \epsilon_k}{\epsilon_i \epsilon_j} ,$$

Table I. Results for LiNbO_3 and LiTaO_3

	LiNbO_3		LiTaO_3	
	28		43	
	43		41	
ϵ_{dc3}	1.8		2.0	
$\epsilon_{dc1,2}$				
ϵ_c^*/ϵ				
	Nb-O (short)	Nb-O (long)	Ta-O (short)	Ta-O (long)
$2r_o$	1.889 Å	2.112	1.891	2.071
f_i	0.821	0.830	0.847	0.853
$-f$	0.292	0.241	0.282	0.238
	r_{33}	r_{51}	r_{33}	r_{51}
r_{ionic}	+19.9	+19.7	+27.8	+16.5
r_{elec}	+ 6.0	+ 0.8	+ 3.70	+ 0.24
r_{theo}	+25.9	+20.5	+31.5	+16.7
r_{sum}				
r_{exptl}	+28	+23	+30	+15

which is equal to 8.55 in CdIn_2Te_4 and to 1.02 in LiNbO_3 . It will be very exciting to see if this prediction is actually true.

We also predict a large EO coefficient for ZnIn_2S_4 since it has 3m symmetry so that the form

$$\sum_{\bar{u}} \alpha_i^u \delta_{jk}$$

is non-vanishing for r_{ijj} . The more numerical prediction awaits the result of measurement of ϵ_{dc} .

REFERENCES

1. A.L. Gentile et. al., this program, Quarterly Report No. 6, August 1979.
2. L. Thomassen et al., J. Electrochem Soc. 110, 1127 (1963); revision by L.I. Berger and V. Prochukhan, Ternary Diamond-Like Semiconductors, Consultants Bureau, New York 1969.
3. D.R. Mason and D.F. O'Kane, Proc. Int. Conf. Semicond. Phys., Prague, 1961, p 1026.
4. S.I. Radautsan, E.K. Arushanov and L.S. Koval, Ternary Compounds $Al^{II}B^{IV}C_2^V$ and $Al^{II}B_2^{III}C_4^{VI}$, Shtiintsa Publishing Co., Kishinev (USSR), 1972, p 217 (in Russian).
5. L.S. Koval, S.I. Radautsan, V.V. Sobolev, Inorganic Materials (USSR) 8 2021 (1972).
6. S.I. Radautsan, L.S. Koval, V.V. Sobolev, and N.N. Syrbu, Ternary Compounds $Al^{II}B^{IV}C_2^V$ and $Al^{II}B_2^{III}C_4^{VI}$, Shtiintsa Publishing Co., Kishinev (1972) p 230 (in Russian).
7. S.V. Bulyarski, L.S. Koval, S.I. Radautsan, Proc. All-Union Conf on Ternary Semiconductors and their applications, Shtiintsa Publishing Co., Kishinev (1976) p 139 (in Russian).

APPENDIX

QUANTITATIVE CALCULATION OF ELECTROOPTIC COEFFICIENTS

The second-order nonlinear optical response of asymmetric crystals is usually represented by the relation $P_i^{(\omega+\Omega)} = \chi_{ijk} E_j^{(\omega)} E_k^{(\Omega)}$ between the amplitude of the induced polarization at $\omega + \Omega$ and the inducing field amplitudes at ω and Ω . The case when both ω and Ω are optical frequencies (i.e., they are frequencies above the lattice response but below the optical absorption) has been considered by Levine.¹ He used the localized bond charge model (see Figure A-1(a)) of Phillips and Van Vechten² (PV), which attributes the dielectric response of covalent crystals to the localized bond charge resulting in a linear susceptibility:

$$\chi = \frac{(\hbar\Omega_p)^2}{E_g^2}, \quad (1)$$

where Ω_p is the plasma frequency due to valence electrons, and E_g (the effective energy gap) is given by $E_g^2 = E_h^2 + C^2$ (where E_h is the homopolar component, and C is the heteropolar (ionic) component of the gap energy). Levine starts with the linear dielectric response $P_i^{(\omega)} = \chi_{ij} E_j^{(\omega)}$, taking χ_{ij} to be an instantaneous function of the second field $E_k^{(\Omega)}$. This field causes a change $\Delta r_\alpha (= -\Delta r_\beta)$ in the bond charge position, as shown in Figure A-1(a), that oscillates at Ω . The explicit dependence of E_g and C on r_α given by PV² is then used to obtain χ_{ijk} , where

$$\chi_{ij} = \chi_{ij}^{(0)} + \Delta\chi_{ij}(t) = \chi_{ij}^{(0)} + 2\chi_{ijk} E_k^{(\Omega)} \cos \Omega t. \quad (2)$$

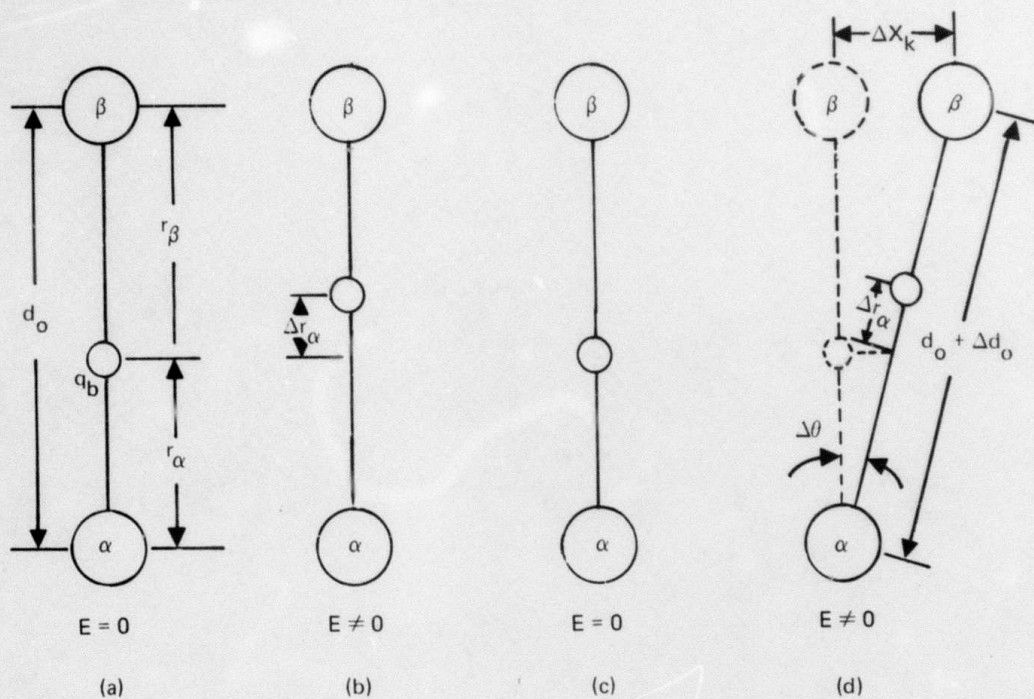


Figure A-1. The response of ion and bond-change to the applied electric field. In (a) and (b) the frequency of the field is higher than the lattice response. Only the displacement of the bond charge takes place. In (c) and (d) the frequency of the field is lower than the lattice response. It induces the displacement of the bond charge (Δr_α), bondlength elongation (Δd_0), and bond rotation ($\Delta \theta$).

If the frequency Ω is below the lattice response region (we will refer to it in this case as "low"), then, in addition to the purely electronic nonlinear response described above, there is now a contribution to χ_{ijk} because the crystalline ions are capable of following the field $E_k^{(\Omega)} \cos \Omega t$. This is illustrated in Figure A-1(c and d). In addition to the displacement Δr_α of the covalent bond charge, there is now an elongation Δd_o of the atomic separation and a rotation θ of the bond direction; these are caused by the ionic displacement Δx_k . Δx_k is obtained from "low" frequency dielectric constant measurements and is used to obtain Δd_o and $\Delta \theta$. We use, in the spirit of Levine,¹ the change Δd_o to calculate the corresponding change $\Delta \chi \cos \Omega t$ in bond susceptibility. This will give rise to a polarization

$$P_i^{(\omega+\Omega)} = \chi_{ijk} E_j^{(\omega)} E_k^{(\Omega)} .$$

A second contribution to χ_{ijk} is due to the rocking at Ω of the bond angle ($\theta = \theta_o + \Delta \theta \cos \Omega t$), which yields a dipole component along i at $(\omega+\Omega)$ even when $\Delta d_o = 0$.

In what follows, we will obtain expressions for the ionic contribution to χ_{ijk} , which is due to Δd_o and $\Delta \theta$. Adding this result algebraically to χ_{ijk}^{elec} (as measured by second harmonic generation experiments or calculated by Levine¹) yields the total nonlinear tensor

$$\chi_{ijk} = \chi_{ijk}^{\text{ionic}} + \chi_{ijk}^{\text{elect}} .$$

The constants χ_{ijk} thus determined are those which characterize the linear electrooptic (Pockels) effect. The relationship between the conventionally defined electrooptic tensor r_{ijk} and χ_{ijk} is (in MKS units)

$$\chi_{ijk} = - \frac{\epsilon_i \epsilon_j}{2\epsilon_0} r_{ijk} . \quad (3)$$

We use this procedure below to calculate the tensor r_{ijk} in a number of zincblende and wurtzite crystals. The results are in good agreement with experiments.

The linear susceptibility of a diatomic crystal is given as $\chi = (h\Omega_p)^2/E_g^2$ (Ref. 2). The ionicity and covalency of the bond are defined as $f_i = C^2/E_g^2$ and $f_c = E_h^2/E_g^2$, respectively. Values of E_h , C , f_c , and f_i for a large number of crystals are given in Ref. 3. The expressions used in the evaluation of E_h and C are^{1,2}

$$E_h \propto r_o^{-s} , \quad s = 2.48 \quad (4)$$

$$C \propto e^{-k_s r_o} \left(\frac{Z_\alpha}{r_\alpha} - \frac{Z_\beta}{r_\beta} \right) e^2 \quad (5)$$

$$r_\alpha \approx r_\beta \approx r_o = \frac{d_o}{2} ,$$

where $d_o = r_\alpha + r_\beta$ is the bond length, $r_{\alpha,\beta}$ are the atomic radii, $e^{-k_s r_o}$ is the Thomas-Fermi screening factor, and the proportional factors in E_h and C are independent of bond length and atomic radius.

To consider the crystals with highly unequal atomic radii, a generalized form for E_h was proposed:¹

$$E_h^{-2} \propto r_o^{2s} \frac{[(r_\alpha - r_c)^{2s} + (r_\beta - r_c)^{2s}]}{2(\Omega_o - r_c)^{2s}} , \quad (6)$$

where r_c is the average core radius, which is included here since the contribution to the susceptibility in the core region is very small.

The linear macroscopic susceptibility tensor χ_{ij} is related to the bond polarizability β_n by

$$\chi_{ij} = \frac{1}{V} \sum_n \alpha_{ni} \alpha_{nj} \beta_n, \quad (7)$$

where V is the volume of the unit cell, α_{ni} is the direction cosine of the bond, n refers to the individual bond, and the summation is over all the bonds in a unit cell. Although PV described the macroscopic susceptibility χ in terms of the average energy gap, we assume that E_h and C should be related to the bond polarizability directly, i.e.,

$$\beta_n \propto \frac{(\hbar \Omega_p)^2}{E_g^2}.$$

The change of bond polarizability due to the applied electric field is

$$\frac{\Delta \beta}{\beta} = \frac{\Delta(\Omega_p^2)}{\Omega_p^2} + f_c E_h^2 \Delta(E_h^{-2}) - 2f_i \frac{\Delta C}{C}. \quad (8)$$

When the bond length varies, it is reasonable to assume that the ratio of r_α to r_β remains constant. With this assumption, the two independent parameters, $r_{\alpha,\beta}$, can be transformed into two quantities that relate directly to the macroscopic properties of crystals:

$$\begin{aligned} \Delta r_\alpha &= \frac{r_\alpha}{d_o} \Delta d_o + \delta \\ \Delta r_\beta &= \frac{r_\beta}{d_o} \Delta d_o - \delta, \end{aligned} \quad (9)$$

where δ is the displacement of the bond charge in the case of no bond elongation $\Delta d_o = 0$. From Eqs. 5, 6, 8, and 9, the change of bond polarizability is obtained as (here we drop the bond index n):

$$\frac{\Delta\beta}{\beta} = \left\{ \left[f_i \left(1 + \frac{k_s r_o}{2} \right) + s f_c - \frac{3}{2} \right] \frac{\Delta d_o}{r_o} + \left[4 f_i \frac{Z_\alpha + Z_\beta}{Z_\alpha - Z_\beta} + s(2s - 1) \frac{f_c \rho d_o^2}{(r_o - r_c)^2} \right] \frac{\delta}{d_o} \right\}, \quad (10)$$

where $\rho = (r_\alpha - r_\beta)/(r_\alpha + r_\beta)$. In the first term, $k_s r_o/2$ is obtained for the screening wave number, k_s is proportional to $d_o^{-1/2}$ (Ref. 4), and the number $(-3/2)$ is due to the fact that Ω_p is proportional to $d_o^{-3/2}$. The second term on the right side of Eq. 10 is exactly the same as the expression obtained by Levine in his calculation of the nonlinear optical susceptibility.⁵ The first term, which is proportional to d_o , is thus the ionic contribution of a single bond due to bond stretching.

The rotational contribution can be obtained by considering the changes in bond direction cosines. These are related to the ionic displacement Δx_k by

$$\Delta\alpha_{ni} = (\delta_{ik} - \alpha_{ni} \alpha_{nk}) \Delta x_k.$$

From Eq. 7 we have

$$\Delta\chi_{ij} = \frac{1}{V} \sum_n (\alpha_{ni} \alpha_{nj} \Delta\beta_n + \Delta\alpha_{ni} \alpha_{nj} \beta_n + \alpha_{ni} \Delta\alpha_{nj} \beta_n). \quad (11)$$

The complete ionic contribution to the nonlinear susceptibility is thus

$$\Delta\chi_{ij}^{\text{ion}} = \left\{ \sum_n \frac{\beta_n}{Vr_o} \left[f\alpha_{ni}\alpha_{nj}\alpha_{nk} + \frac{1}{2} (\alpha_{nk}\delta_{jk} + \alpha_{nj}\delta_{ik}) \right] \right\} \Delta x_k, \quad (12)$$

where

$$\begin{aligned} f &= f_i \left(1 + \frac{k_s r_o}{2} \right) + sf_c = 2.5 \\ &= \left(\frac{k_s r_o}{2} - 1.48 \right) f_i - 0.02. \end{aligned} \quad (13)$$

Δx_k is related to the dielectric constant of the crystal as

$$Ne_c^* \Delta x_k = \epsilon_o (\epsilon'_{dc} - \epsilon'_\infty) E_k^s, \quad (14)$$

where N is the number of pairs of atoms per unit cell, e_c^* is the Callen effective ionic charge,⁶ ϵ'_{dc} is the relative dielectric constant, ϵ'_∞ is the relative optical permittivity, and E_k is the low-frequency electric field component along the k direction.

Using Eq. 3 we obtain the final working expression for the electro-optic tensor:

$$r_{ijk}^{\text{ion}} = - \frac{\epsilon_o (\epsilon'_{dc} - \epsilon'_\infty)}{VNe_c^* \epsilon'_i \epsilon'_j} \left\{ \sum_n \frac{\beta_n}{r_o} \left[f\alpha_{ni}\alpha_{nj}\alpha_{nk} + \frac{1}{2} (\alpha_{ni}\delta_{jk} + \alpha_{nj}\delta_{ik}) \right] \right\}. \quad (15)$$

For wurtzite crystals, we neglect the small distortion from the perfect tetragonal structure. β_n can be expressed in terms of the measured macroscopic susceptibility χ as in Eq. 7, and the electrooptic coefficients of zincblende and wurtzite crystals are obtained as follows:

$$\text{zincblende } r_{14}^{\text{ion}} = 0.3689 \frac{a_o^2 w f}{e_c^*/e} \quad (16)$$

$$\text{wurtzite } r_{33}^{\text{ion}} = -2 r_{13}^{\text{ion}} = 0.4260 \frac{a_{\text{eff}}^2 w f}{e_c^*/e}, \quad (17)$$

where a_o is the lattice constant; $a_{\text{eff}} = \sqrt{3} a_o^2 c_o$; $w = (\epsilon - 1)(\epsilon_{\text{dc}} - \epsilon)/\epsilon^2$; the r_{ij} are in units of 10^{-12} m/V; and a_o , a_{eff} are in units Å. Values of the parameters a_o , a_{eff} , w , f_i , f , and e_c^* are listed in Table A-I.

The dependence of the electrooptic coefficients r_{ijk}^{ion} on the bond geometry is perhaps the most illuminating feature to emerge from this work. This dependence is contained in curly brackets in Eq. 15. For diatomic single-bond crystals, β_n is a constant, and the geometrical factor becomes

$$G_{ijk} = \sum_{\text{bonds } n} \left[f \alpha_{ni} \alpha_{nj} \alpha_{nk} + \frac{1}{2} (\alpha_{nk} \delta_{jk} + \alpha_{nj} \delta_{ik}) \right].$$

The factor f is typically $|f| \leq 0.3$. Table A-II contains a listing of these factors for some key directions (ijk) in crystals of the zincblende, wurtzite, and LiNbO_3 classes.

It follows immediately that when $\sum_n \alpha_{ni} \neq 0$ the second term in G_{ijk} is an order of magnitude larger than the first one. In such crystals, the ionic contribution to r_{ijk} is about an order of magnitude larger

Table A-I. Parameters and Results of EO Calculations

AB	Zincblende						Wurzite		
	GaAs	GaP	ZnSe	ZnS	ZnTe	CuCl	ZnS	CdS	CdSe
a^a	5.65	5.45	5.67	5.41	6.09	5.41	5.39	5.85	6.08
ϵ_{dc}	13.2 ^b	12.0 ^c	9.1 ^d	8.3 ^d	10.1 ^d	7.5 ^e	8.7 ^f	9.4 ^d	10.2 ^d
w	0.192	0.284	0.450	0.528	0.331	0.656	0.567	0.652	0.562
f_i^g	0.310	0.370	0.630	0.623	0.546	0.749	0.623	0.683	0.699
f	-0.091	-0.113	-0.163	-0.179	-0.119	-0.212	-0.181	-0.162	-0.147
e_c^*/e	0.20	0.23	0.33	0.35	0.26	0.27	0.35	0.41	0.36
r_{ionic}	+1.03	+1.53	+2.64	-2.93	+2.07	-5.56	+3.63	+3.75	+3.61
r_{elec}	-2.73 ^h	-3.20 ⁱ	-4.68 ^j	-4.77 ^k	-6.41 ^l	+2.66 ^m	-5.63 ^k	-6.71 ^k	-7.40 ^j
r_{theo}	-1.7	-1.7	-2.0	-1.8	-4.3	-2.9	-2.0	-3.0	-3.8
r_{exptl}	-1.6 ^h	-1.1 ⁿ	2.0 ^c	1.6 ^c	4.3 ^c	-2.4 ^c	1.8 ^c	3.0 ^c	4.3 ^c

NOTE: $a = a_o$ or a_{eff} . r 's represent r_{14} (zincblende) and r_{33} (wurtzite) and are in units of 10^{-12} m/V. r_{exptl} are measurements with clamped crystals. Their signs have not been determined unless specified.

- a. R.W.G. Wyckoff, "Crystal Structures," 2nd ed. Vol. 1 (1963).
- b. S. Jones and S. Mao, J. Appl. Phys. 39, 4038 (1968).
- c. I.P. Kaminow and E.H. Turner, Proc. IEEE 54, 1374 (1966).
- d. D. Berlincourt, H. Jaffe, and L.R. Shiozawa, Phys. Rev. 129, 1009 (1963).
- e. P. Alomas, G. Sherman, C. Wittig, and P.D. Coleman, Appl. Optics 8, 2557 (1968).
- f. I.B. Kobaykov, Soviet Phys.-Cryst. 11, 369 (1966)
- g. J.A. Van Vechten, Phys. Rev. 182, 891 (1969); 187, 1007 (1969).
- h. A. Mooradian and A.L. McWhorter, "Light Scattering Spectra of Solids," G.B. Wright, ed. (Springer, New York, 1969).
- i. J.J. Wynne and N. Bloembergen, Phys. Rev. 188, 1211 (1969).
- j. R.A. Soref and H.W. Moos, J. Appl. Phys. 35, 2152 (1964).
- k. C.K.N. Patel, Phys. Rev. Lett. 16, 613 (1966).
- l. R.K. Chang, J. Ducuing, and N. Bloembergen, Phys. Rev. Lett. 15, 415 (1965).
- m. D. Chemla, P. Kupecek, C. Schwartz, C. Schwab, and A. Goltzene, IEEE J. Quant. Electron. 7, 126 (1971).
- n. D.F. Nelson and E.H. Turner, J. Appl. Phys. 39, 3337 (1968).

Table A-II. Comparison of the Geometrical Factors Between
Zincblende and Wurtzite and LiNbO_3

	Zincblende	Wurtzite	LiNbO_3	
			(Nb-O) Short	(Nb-O) Long
$\sum_i \alpha_{n3}$	0	0	2.849	-4.014
$\sum_n \alpha_{ni}^2$	16/3	8/3	2.0	2.0
$\sum_i \alpha_{n1} \alpha_{n2} \alpha_{n3}$	$16/3 \sqrt{3}$	0	0	0
$\sum_n \alpha_{n1}^2 \alpha_{n3} = \sum_n \alpha_{n2}^2 \alpha_{n3}$	0	-8/9	1.103	-1.109
$\sum_n \alpha_{n3}^3$	0	16/9	0.642	-1.797
$\sum_n \alpha_{n2}^3$	0	0	0.396	-0.195

than the electronic term. This is the case in LiNbO_3 and LiTaO_3 . When $\sum_n \alpha_{ni} = 0$, as in zincblende and wurtzite, we have to settle for the smaller term $\sum_n f \alpha_{ni} \alpha_{nj} \alpha_{nk}$. This is the main reason why LiTaO_3 has $r_{33} = 30.3 \times 10^{-12} \text{ m/V}$, while GaAs and ZnS have $r_{41} \approx 2 \times 10^{-12} \text{ m/V}$.

The effective charge e_c^* is related to the Szigetti effective charge e_s^* by

$$e_c^* = \frac{\epsilon_\infty + 2}{3\epsilon_\infty} e_s^* .$$

The value of e_c^* varies from 0.2 to 0.4 and seems to be independent of the number of valence electrons. The calculation of r_{ijk}^{ion} using Eqs. 17 and 18 is shown in Table I as r_{ionic} . The pure electronic contribution is entered as r_{elec} . It is obtained directly from the second harmonic generation coefficient by $r_{\ell k} = -4d_{\ell k}/\epsilon^2$. For most of the crystals in Table I, r_{ionic} is positive and r_{elec} is negative. Therefore, the predicted electrooptic coefficients, $r_{\text{sum}}^{\text{theo}} = r_{\text{ionic}} + r_{\text{elec}}$, involve the algebraic addition of two numbers of comparable values. The only exception is CuCl. Due to the unfilled shell in Cu, the sense of bond polarization in CuCl is different from that in other crystals.⁷ For example, excluding valence electrons, As is +5, Ga is +3, and Cl is +7, but Cu is +11. So the signs of r_{ionic} and r_{elec} of CuCl are different from those of other crystals. However, since the magnitude of r_{ionic} is larger than that of r_{elec} in CuCl, we still obtain a negative electrooptic coefficient for CuCl. Predicted values in Table I show a good agreement with experiment. The worst case is GaP. It is interesting to note that the electronic contribution is about double the ionic contribution. This is in excellent agreement with the experimental observation.⁸

We find that the contributions to r_{ijk} from the homopolar part and the heteropolar part are comparable. We intend to extend this model to complex crystals with different point group symmetries. The generalization of the bond parameters used above to multibond crystals has already

been considered. The one parameter that will need consideration is e_s^* , the effective ionic charge. It was found empirically to be equal to $C/\kappa\omega_p$ in diatomic crystals.⁹ If this relation and

$$e_c^* = \frac{\epsilon_\infty + 2}{3\epsilon_\infty} e_s^*$$

are valid in the more complex crystals, then our model can be applied to these cases. Present calculations on LiNbO_3 , LiTaO_3 , and ternary chalcopyrite crystals are reported in this document (see Table I).

REFERENCES

1. B.F. Levine, Phys. Rev. Lett. 22, 787 (1969); 25, 440 (1970).
2. J.C. Phillips, Phys. Rev. Lett. 20, 550 (1968).
3. J.A. Van Vechten, Phys. Rev. 182, 891 (1969); 187, 1007 (1969).
4. C. Kittel, Introduction to Solid State Physics, 5th ed. (John Wiley, N.Y., 1976).
5. B.F. Levine, Phys. Rev. B7, 2600 (1973).
6. H.B. Callen, Phys. Rev. 76, 1394 (1949).
7. I.P. Kaminow and E.H. Turner, Phys. Rev. B5, 1564 (1972).
8. W.L. Faust and C.H. Henry, Phys. Rev. Lett. 17, 1265 (1966).
9. P. Lawaetz, Phys. Rev. Lett. 26, 697 (1971).